Electronic Supplementary Material (ESI) for ChemComm.
This journal is © The Royal Society of Chemistry 2019

ChemComm
Chemical Communications
www.rsc.org/chemcomm

Supporting Information

Three thymine-adenine binding modes of the ruthenium complex Λ-$[Ru(TAP)_2(dppz)]^{2+}$ to the G-quadruplex d(TAGGGTT) shown by X-ray crystallography

Kane McQuaid,[a,b] James P. Hall,[b,c] Lena Baumgartner,[a] David J. Cardin[a] and Christine J. Cardin*[a]

[a] Department of Chemistry, University of Reading, Whiteknights, Reading, Berkshire, RG6 6AD, UK
[b] Diamond Light Source Ltd., Harwell Science and Innovation Campus, Didcot, Oxfordshire, OX11 0DE, UK
[c] Department of Pharmacy, University of Reading, Whiteknights, Reading, Berkshire, RG6 6AP, UK
Email: c.j.cardin@reading.ac.uk

1. Experimental

1.1. Materials

Oligonucleotides were purchased from Eurogentec as HPLC-purified solids and were used without further purification. Unless otherwise stated, all other materials and chemicals were sourced from Sigma Aldrich or Honeywell research chemicals. Sephadex C-25 anion exchange stationary phase and Dowex 1X2 Chloride form anion exchange resin were purchased from GE Healthcare. All solvents, unless stated in the experimental, were obtained at HPLC grade and used without further purification. Where further purification was needed, protocol from "Purification of Laboratory Chemicals, 4th edition, Armarego *et. al.*" was followed. Deuterated solvents for NMR analysis were purchased either through Sigma-Aldrich or Cambridge Isotope Laboratories.

1.2. Instrumentation

Unless otherwise stated, all ^{1}H NMR spectra were collected on a Bruker Nanobay 400 MHz instrument, with the majority of ^{13}C NMR spectra collected on a Bruker DPX 400.1 MHz machine operating at 100.1 MHz. Both machines were calibrated against a tetramethylsilane (TMS) internal standard and have two channels running TOPSPIN 2.4 and ICON NMR 4.2. All *J*-coupling constants were reported following normalisation against the used Larmor frequency, where a few couplings were omitted subject to spectral resolution.

High resolution ESI mass spectra were recorded on a Thermo Scientific LTQ Orbitrap XL running in positive ion mode. Fragmented Ions were detected on an Orbitrap Ion trap photodiode array detector and were determined via peak matching against the internally calibrated lock mass for Diisooctyl phthalate (*m/z* = 413.26623). Data analysis was performed on the Xcalibur Qual Browser software package and all accurate masses are reported within 3 ppm.

1.3 Synthesis

1.3.1 dipyridophenazine (dppz)

As described in the literature, dipyridophenazine was synthesised via an acid-catalysed condensation of phendione and 1,2-phenylenediamine. A well-mixed ethanolic solution (15 mL) of phendione (0.515 g, 2.45 mmol) was added slowly to an ethanolic solution (10 mL) of phenylenediamine (0.53 g, 4.91 mmol) with a trace amount of *ρ*-toluene sulfonic acid. The suspension was refluxed for 3 hours before removing the condenser and allowing approximately half of the ethanol to evaporate. The remaining suspension was cooled to room temp and a brown precipitate was observed. The solid was collected via suction filtration, washed with cold ethanol (2 x 5 mL) and recrystallized from aqueous ethanol (1:1) to yield the target product as ochre needle-like crystals (0.569 g, 1.93 mmol, 82 %)

δ_H (400 MHz, TMS, $CDCl_3$-*d*) – 9.68 (dd, *J* = 8.1, 1.8 Hz, 2H), 9.29 (dd, *J* = 4.5, 1.8 Hz, 2H), 8.39 (dd, *J* = 6.5, 3.4 Hz, 2H), 7.94 (dd, *J* = 6.5, 3.4 Hz, 2H) and 7.82 ppm (dd, *J* = 8.1, 4.5 Hz, 2H). **δ_C (101 MHz, $CDCl_3$-*d*) –** 152.58, 148.44, 142.51, 141.17, 133.79, 130.68, 129.57, 127.61 and 124.16 ppm. **HRMS-ES (m/z) –** Found ($[M+H]^+$, 283.0979); calc. 282.0978 ($C_{18}N_4H_{11}^+$).

1.3.2 Ruthenium bis-(tetraazaphenanthrene) dipyridophenazine dichloride (rac-[Ru(TAP)$_2$(dppz)]·Cl$_2$)

The synthesis of *rac*-[Ru(TAP)$_2$(dppz)]·Cl$_2$ has been described by us before and is based on a modified procedure published by Kirsch-DeMesmaeker *et al*.[1,2] Ru(TAP)$_2$Cl$_2$ (81 mg, 0.15 mmol) and dppz (42 mg, 0.15 mmol) were both suspended together in an aqueous ethanol solution (7 mL, 1:1) within a CM microwave tube (10 mL). The violet coloured solution was degassed/evacuated with Ar for 15 minutes before being fully sealed and installed into the synthetic microwave. The sample was irradiated at 140W at 60^{o}C for 40 minutes, yielding a deep red/brown solution which was cooled and then filtered *in vacuo*. Subsequent precipitation of the target compound from the filtrate was achieved by metathesis via dropwise addition of a saturated solution of aqueous potassium hexafluorophosphate (KPF$_6$). Isolation of the PF$_6^-$ salt by *in vacuo* filtration yielded a dark orange/brown solid, which, after washing with cold water (2 x 2 mL) was allowed to dry in air. Conversion to the chloride form was performed through the dissolution of the crude material in a minimal amount of acetonitrile (~5 mL), addition of HPLC grade water (10 mL) to a beaker of dry, washed, Amberlite ion exchange resin (IRA-400, Cl$^-$ form, 2.4 g), covering and lightly stirring for 20 hours. Following removal of the resin by gravity filtration, the complex was isolated via rotary evaporation and purified via flash chromatography on an aqueous Sephadex C-25 column using 0.2M aqueous NaCl as the mobile phase (eluting as a deep orange/red band). The collected aliquots were combined and desalted via metathesis to the hexafluorophosphate salt and finally treated with Amberlite resin (IRA-400, Cl$^-$ form, 2.4 g) as described before, to yield the complex as a deep red/brown microcrystalline solid (88 mg, 0.11 mmol, 74 %).

δ_H (400 MHz, TMS, CD$_3$CN-*d*$_3$) – 9.67 (dd, J = 8.2, 1.3 Hz, 2H), 8.90 (dd, J = 9.6, 2.8 Hz, 4H), 8.55 (s, 4H), 8.42 (dd, J = 6.6, 3.4, 2H), 8.23 (d, J = 2.8 Hz, 2H), 8.17 (d, J = 2.8 Hz, 2H), 8.13-8.06 (m, 4H) and 7.77 ppm (dd, J = 8.3, 5.4 Hz, 2H). **δ_C (101 MHz, H$_2$O-*d*$_2$) –** 151.85, 147.79, 146.81, 146.62, 146.34, 143.00, 140.55, 140.48, 137.50, 133.45, 130.84, 130.63, 130.58, 128.89, 126.95, 125.41 and 124.93 ppm. **HRMS-ES (m/z) —** Found (M$^+$, 374.0559); calc. 374.0561 (RuC$_{38}$N$_{12}$H$_{22}^{2+}$)

1.4 Macromolecular X-ray Crystallography

1.4.1 rac-[Ru(TAP)$_2$(dppz)]$^{2+}$ with d(TAGGGTT)

1.4.1.1 Crystallisation Parameters

Crystals containing the oligonucleotide d(TAGGGTT) and the ruthenium complex [Ru(TAP)$_2$(dppz)]$^{2+}$ were grown from sitting drops via vapour diffusion of water at 18 ^{o}C. Crystals suitable for X-ray diffraction experiments were obtained from various differing conditions from a Natrix HT screen, however not all conditions gave rise to well diffracting samples. The solution forming the sitting drops constituted of two components; 1µL of a pre-annealed mixture of the single stranded oligonucleotide at 250 µM with the complex *rac*-[Ru(TAP)$_2$(dppz)]Cl$_2$ at 250 µM in a 100 mM KCl buffer; and 1 µL of a solution containing 35% v/v Tacsimate™ pH 6.0 and 1 mM spermine; buffered to pH 6.0 using 50 mM sodium cacodylate trihydrate. The sitting drop was equilibrated against 100 µL of the latter solution containing Tacsimate™, spermine and sodium cacodylate trihydrate, forming small dark orange/red hexagonal rods within 2 weeks of preparation.

1.4.1.2 Data Collection and Structure Solution

The data were collected at Diamond Light Source Ltd., on beamline I03 using radiation with a wavelength of 0.5570 Å from a flash cooled crystal at 100K. 360° of data were collected with an oscillation of 0.1° per frame, generating 3600 images. The resulting data were processed using DIALS[3] and Aimless[4] through the xia2[5] pipeline and gave an anomalous signal with a mid-slope of anomalous normal probability[6] of 1.246, finding 8849 unique reflections to a resolution of 1.88 Å. The structure was solved using the anomalous scattering of ruthenium by single wavelength anomalous dispersion using Hybrid Substructure Search (HySS) and Phaser-EP in the PHENIX software package.[7–9] The crystallographic model was built using WinCoot[10] and refined using Phenix.refine[11] to give a final R_{work} of 0.1872 and an R_{free} of 0.2145 reserving 5% of the total reflections for the R_{free} set. Figures were produced using the pymol software suite. The structure is deposited in the Protein Data Bank with PDB accession ID: **6RNL**. Table S1 highlights the main data collection and refinement statistics.

2.1 Table S1 – Crystallisation and data collection parameters

Crystallisation Parameters	
Crystal Morphology	Hexagonal Rod
Growth Temperature (K)	291
Crystal Size (µm)	20x20x300
Growth Time	3 weeks
Data Collection	
Beamline	I03
X-Ray Wavelength (Å)	0.557
Transmission (%)	40.01
Beamsize (µm)	50x20
Exposure Time (s)	0.05
Nº Images/Oscillation (°)	3600/0.10
Space Group	$P\,6_5$
Cell Dimensions *a*, *b*, *c* (Å)	38.53, 38.53, 128.77; 90, 90, 90
Data Processing	
Resolution (Å)	32.29 - 1.88 (1.91 - 1.88)
R_{merge}	0.120 (3.986)
R_{meas}	0.1233 (3.986)
R_{pim}	0.027 (1.003)
Nº Observations	175,231 (7823)
Nº Unique Observations	8849 (465)
I/σI	14.3 (0.7)
$CC_{1/2}$	0.999 (0.585)
Completeness (%)	100.00 (100.00)
Multiplicity	19.8 (16.8)
Mid-slope of anom normal probability	1.246

* Outer Shell Statistics Shown in Parentheses

Refinement	
Phase Solution Method	SAD
Resolution	32.3 - 1.88
No. of Reflections	8708
R_{work}/R_{free}	0.1872/0.2145
No. of Atoms	
DNA	576
Metal Complex	204
Water	75
Average B Factors (Å^2)	
DNA	44.16
Metal Complex	42.62
Water	40.21
rmsd	
Bond Lengths (Å)	0.013
Bond Angles (o)	1.0
PDB ID	**6RNL**

2.2 Figure S1 - $2F_o$-F_c electron density maps of 6RNL

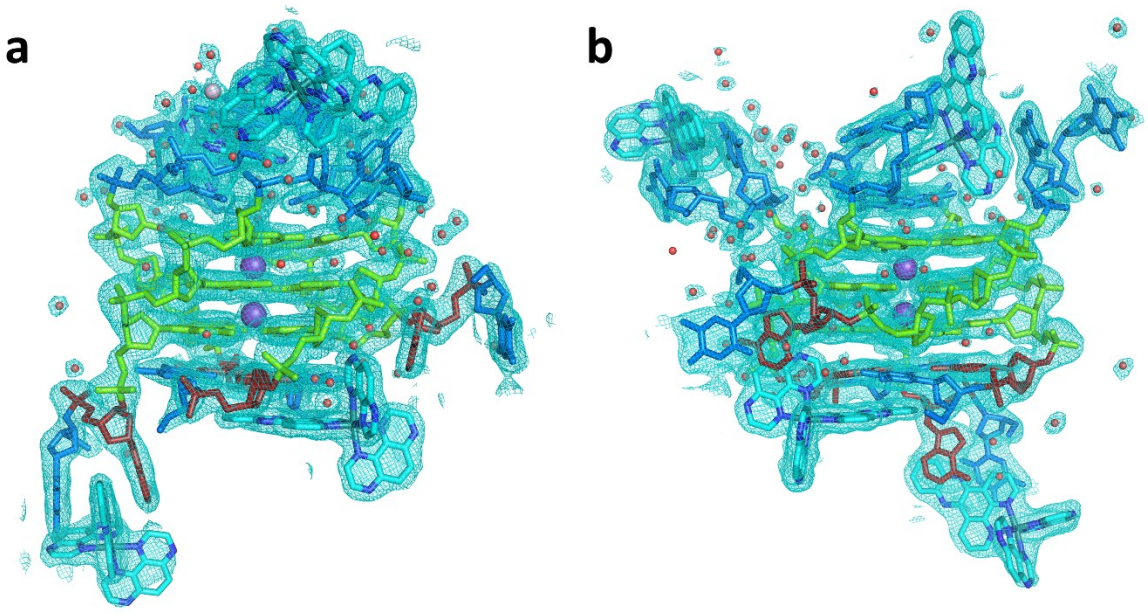

***Figure S1** – Asymmetric unit of **6RNL** illustrating the $2F_o$-F_c electron density map contoured at 0.29 e A^{-3}, viewed from two different orientations (a and b) that are 90^o apart by the helical axis. Residues are coloured using standard nucleic acid database colour scheme where adenine is red, guanine is green, and thymine is blue. Ruthenium complexes are shown as cyan stick models. Potassium ions are depicted by purple spheres, sodium by pink spheres, and waters as red spheres.*

2.3 Figure S2 - Asymmetric unit of 6RNL highlighting the water network of the structure in two different orientations.

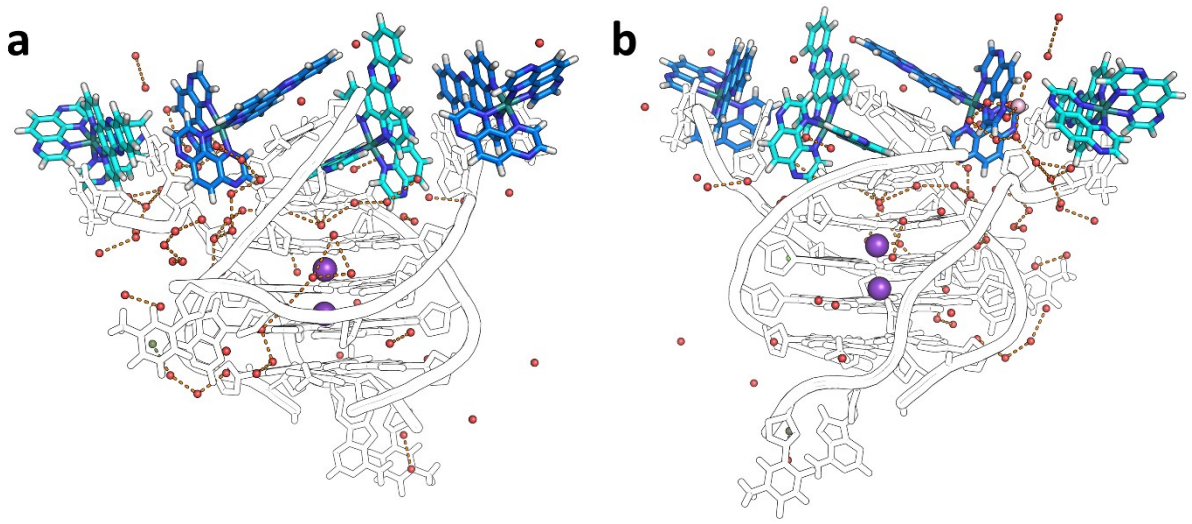

***Figure S2** – Asymmetric unit of **6RNL** highlighting the water network of the structure in two different orientations of the structure (180° about the helical axis). Λ-[Ru(TAP)$_2$(dppz)]$^{2+}$ complexes are coloured in cyan or marine blue. Water molecules are shown as red spheres with local hydrogen bonds shown as dashed bonds. Potassium ions are coloured in purple.*

2.4 Figure S3 – Complex binding modes shown in two orientations highlighting the interactions between neighbouring crystallographically related units.

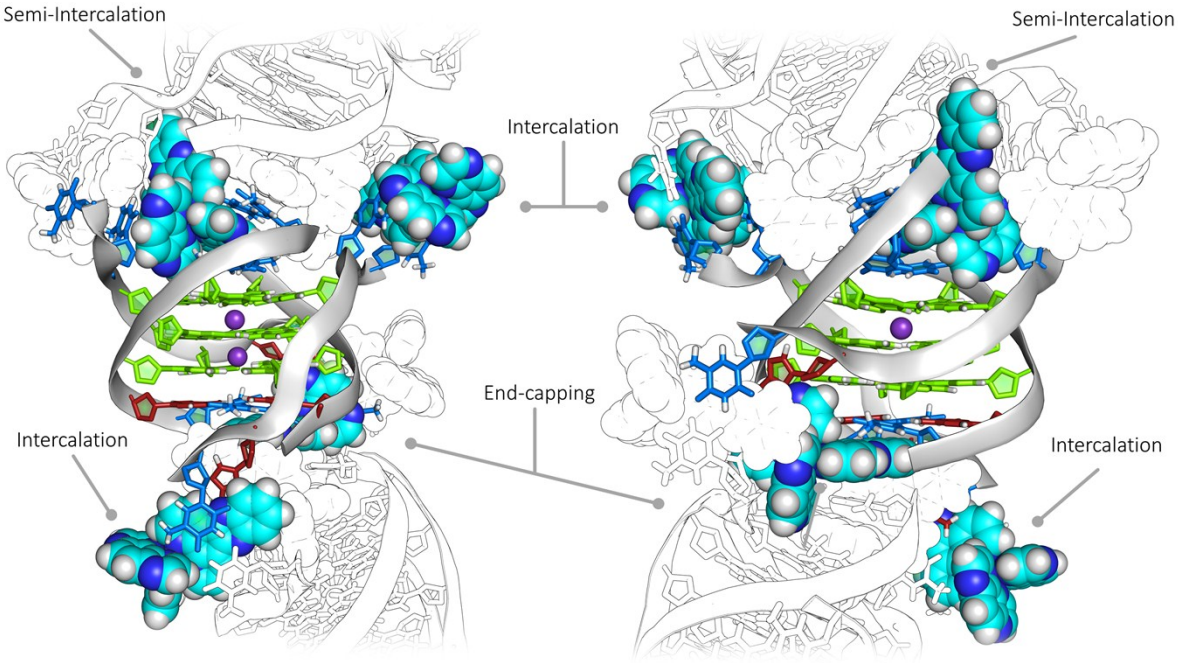

Figure S3 *– The binding modes of ruthenium complexes observed in the structure; highlighting the interactions between neighbouring crystallographically related units. Two views of these interactions are shown and are related by 180º turn about the helical axis. Adenine bases are shown in red, guanine in green, and thymine in blue. Ruthenium complexes are shown as cyan space-filling models. Potassium ions are shown as purple spheres. For clarity, the neighbouring crystallographic units are not coloured.*

2.5 Figure S4 – Projection of the crystal packing down the b axial direction.

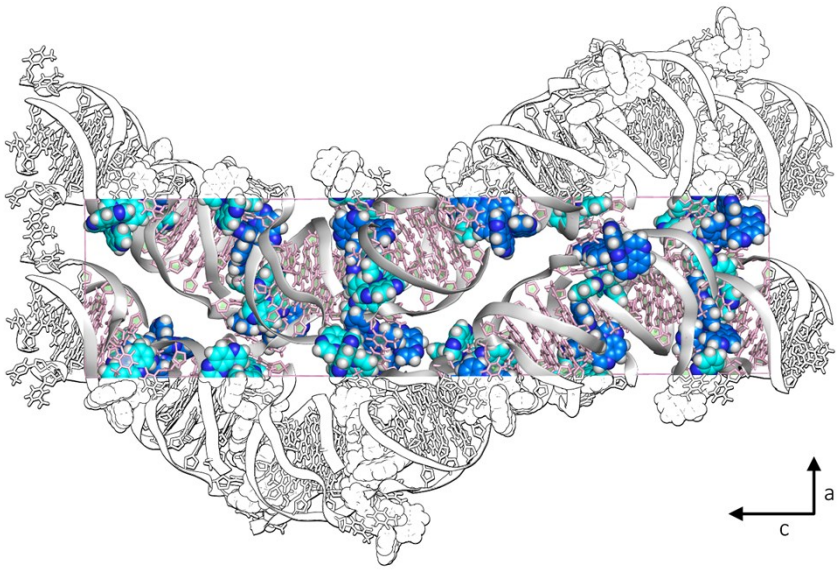

Figure S4 *– Projection of the crystal packing as viewed down the b axial direction of the lattice. All ruthenium complexes are coloured in either cyan or marine. DNA backbone is coloured in silver, with the rest of the nucleosides coloured in pink. Waters have been omitted for clarity. Everything within one unit cell is coloured, whilst the rest is uncoloured.*

2.6 Figure S5 – Projection of the crystal packing down the c axial direction.

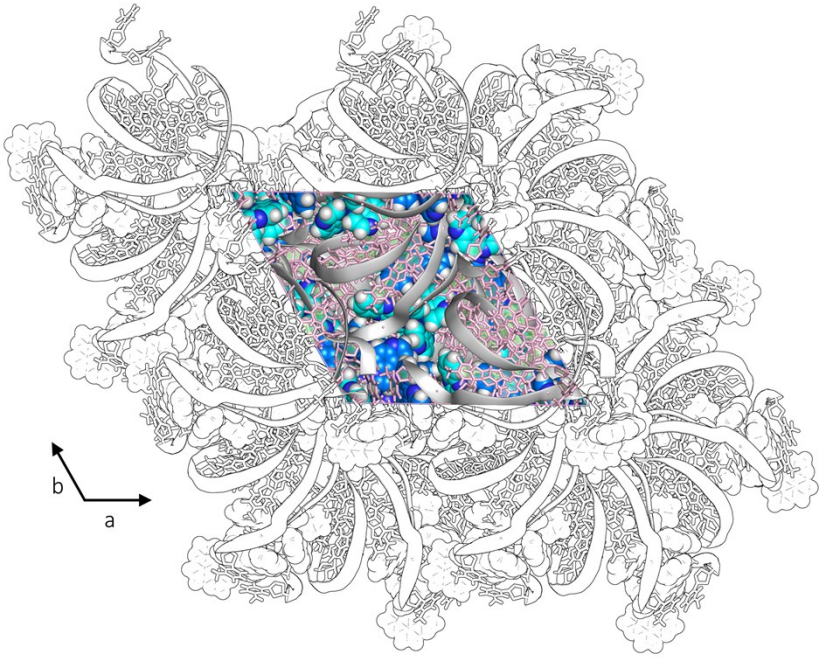

Figure S5 *– Projection of the crystal packing as viewed down the c axial direction of the lattice. All ruthenium complexes are coloured in either cyan or marine. DNA backbone is coloured in silver, with the rest of the nucleosides coloured in pink. Waters have been omitted for clarity. Everything within one unit cell is coloured, whilst the rest is uncoloured.*

3 References

1. Hall, J. . *et al.* Structure determination of an intercalating ruthenium dipyridophenazine complex which kinks DNA by semiintercalation of a tetraazaphenanthrene ligand. *Proc.Natl.Acad.Sci.USA* **108**, 17610–17614 (2011).

2. Ortmans, I., Elias, B., Kelly, J. M., Moucheron, C. & Kirsch-DeMesmaeker, A. [Ru(TAP)2(dppz)]2+: a DNA intercalating complex, which luminesces strongly in water and undergoes photo-induced proton-coupled electron transfer with guanosine-5[prime or minute]-monophosphate. *Dalt. Trans.* 668–676 (2004). doi:10.1039/B313213G

3. Waterman, D. G. *et al.* The DIALS framework for integration software. *CCP4 Newslett. Protein Crystallogr* **49**, 13–15 (2013).

4. Evans, P. Scaling and assessment of data quality. *Acta. Crystallogr.* **D62**, 72–82 (2006).

5. Winter, G., Lobley, C. M. C. & Prince, S. M. Decision making in xia2. *Acta. Crystallogr.* **D69**, 1260–1273 (2013).

6. Howell, P. L. & Smith, G. D. Identification of heavy-atom derivatives by normal probability methods. *J. Appl. Cryst.* 25, 81–86 (1992).

7. Grosse-Kunstleve, R. W. & Adams, P. D. Substructure search procedures for macromolecular structures. *Acta Crystallogr. Sect. D* 59, 1966–1973 (2003).

8. McCoy, A. J. *et al.* Phaser crystallographic software. *J. Appl. Crystallogr.* 40, 658–674 (2007).

9. Adams, P. D. *et al.* PHENIX: A comprehensive Python-based system for macromolecular structure solution. *Acta Crystallogr. Sect. D Biol. Crystallogr.* 66, 213–221 (2010).

10. Emsley, P., Lohkamp, B., Scott, W. G. & Cowtan, K. Features and development of Coot. *Acta. Crystallogr.* D66, 486–501 (2010).

11. Adams, P. D. *et al.* The Phenix software for automated determination of macromolecular structures. *Methods* 55, 94–106 (2011).